

This is the author's peer reviewed, accepted manuscript. However, the online version of record will be different from this version once it has been copyedited and typeset.
PLEASE CITE THIS ARTICLE AS DOI: 10.1063/1.50052142

Explosive crystallization of sputter-deposited amorphous germanium films by irradiation with an electron beam of SEM-level energies

R. Nakamura^{1,a}, A. Matsumoto¹, M. Ishimaru²

¹Department of Materials Science, Graduate School of Engineering, Osaka Prefecture University, Gakuen-cho 1-1, Naka-ku, Sakai 599-8531, Japan

²Department of Materials Science and Engineering, Kyushu Institute of Technology, Tobata, Kitakyushu, Fukuoka 804-8550, Japan

^aE-mail: nakamura@mtr.osakafu-u.ac.jp

Abstract

The crystallization of sputter-deposited substrate-free films of amorphous germanium (a-Ge) was induced by electron irradiation at SEM-level energies of less than 20 keV at ambient temperature using an electron probe microanalyzer. Instantaneous crystallization, referred to as explosive crystallization, occurred consistently at 2~20 keV; threshold of electron fluxes is $10^{15} - 10^{16} \text{ m}^{-2} \text{ s}^{-1}$, which are five to six orders of magnitude lower than those at 100 keV reported previously. This process is expected to be advantageous in the production of polycrystalline Ge films since it is rapid, requires little energy, and results in negligible damage to the substrate.

1. Introduction

Thin films of polycrystalline silicon (Si), germanium (Ge) and their alloys are leading materials in electronic devices because of high carrier mobilities and low energy-band-gap.¹⁻⁴⁾ The production of polycrystalline films generally involves two steps: amorphous films are deposited on glass substrates and then are crystallized by conventional furnace-heating,^{5,6)} laser annealing,⁷⁻⁹⁾ or flash-lamp annealing.^{2,10)} Recent efforts to develop low-temperature processes to reduce energy costs are also expanding the selection of substrate available. The feasibility of using polycrystalline thin films comprised of polymers for flexible devices is now actively researched.

In a series of our studies¹¹⁻¹⁴⁾ on crystallization behavior of sputter-deposited amorphous films of Ge (a-Ge), we demonstrated by transmission electron microscopy that the irradiation using an electron-beam with 100 keV of energy induces rapid crystallization at room temperature. Crystal growth occurred instantaneously beyond 50 μm in diameter when irradiating using an electron beam 1 μm in diameter.¹⁴⁾ This behavior is referred to as explosive crystallization (EC),¹⁵⁾ and is known to be triggered by instantaneous processes such as mechanical stimulation,¹⁵⁾ laser irradiation,¹⁶⁾ electron-beam heating,¹⁷⁾ and flash-lamp annealing.¹⁸⁾ Electron irradiation at low energy levels has potential to facilitate rapid and extensive crystallization of a-Ge films in a low temperature range, therefore avoiding thermal damage to substrate.

It is not the elastic interactions between electrons and atoms that results in the crystallization of a-Ge by electron irradiation. Rather, crystallization occurs due to the electronic excitation effects (ionization effects)¹⁹⁻²¹⁾, which involve the breaking and rearrangement of unstable bonds. It is considered likely that the effects of electronic excitation effects more efficiently induce an atomic event as electron energy becomes lower. The first aim of this study is, therefore, to attempt to

demonstrate the EC of a-Ge by irradiation of electron of energies below 20 keV in a scanning electron microscope.

In an earlier study by our group,¹⁴⁾ it was found that EC occurred in pristine films but did not occur in films aged at room temperature for 6 months or longer. We proposed a mechanism for EC¹⁴⁾ by considering the structural features of a-Ge¹¹⁾. We determined that the sputter-deposited films initially contain medium-range ordered (MRO) clusters, and that the rapid growth of those clusters is facilitated by the rapid stimulation of the fluid interface of a liquid-like, high-density amorphous²²⁻²⁴⁾ state. Stimulation is typically provided in the form of electron irradiation at 100 keV and flash-lamp annealing. This mechanism does not appear to occur in samples stabilized by aging at room temperature for over 6 months when subject to electron irradiation of 100 keV. This may be because of the decrease in the number and size of MRO clusters and the release of strain is released during the aging process. The effects of aging at room temperature on the crystallization behavior of samples subject to low-energy electron irradiation were investigated in this study.

2. Experimental procedure

2.1. Sample preparation

Thin films of amorphous Ge (a-Ge) of a thickness of 40 nm were prepared by radio-frequency (RF) sputtering at a base pressure below 3×10^{-5} Pa. A polycrystalline Ge with a purity of 99.99% and a diameter of 101.6 mm was used as the target. Cleaved crystals of sodium chloride (NaCl) with dimensions of about $4 \times 4 \times 2$ mm³ were used as the substrate. Thin films were deposited on the clean surface of the substrates kept at the ambient temperature by sputtering the target under a RF output power of 50 W and in a stream of argon of 0.7-0.8 Pa. The films deposited on the substrates were aged for either two weeks or 30 months: the former and latter are hereafter referred to as “pristine” and “aged” samples, respectively. The aged samples were kept in a transparent desiccator where the

temperature and humidity were kept at $20\text{ }^{\circ}\text{C} \pm 5\text{ }^{\circ}\text{C}$ and below 40%, respectively, at atmospheric pressure. The films on the substrates were placed in distilled water, and then the floating films were recovered on copper (Cu) grids with a hole size of $100 \times 100\text{ }\mu\text{m}^2$.

2.2. Electron irradiation and observation

The samples were irradiated with an electron beam with 1 - 20 keV of energy at room temperature in an electron probe microanalyzer (EPMA, JEOL JXA-8530F). The current of the incident electron-beam was monitored using a Faraday cage of 62.2 mm^2 . The maximum flux of electrons output by the EPMA was between 1×10^{15} and $1 \times 10^{17}\text{ m}^{-2}\text{ s}^{-1}$ under an acceleration voltage of 1 and 20 kV, respectively.

The diameter of focused electron beam was less than $1\text{ }\mu\text{m}$. We can specify the scanning area of the electron beam at $n \times n\text{ }\mu\text{m}^2$ (n is whole number), as a function of the concentration-analysis mode of the EPMA. To determine whether EC occurred or not, the scanning area was changed from the minimum, $1 \times 1\text{ }\mu\text{m}^2$. It was found that EC was induced at least at $8 \times 8\text{ }\mu\text{m}^2$, and then the irradiation area was fixed at these values.

The microstructure of the irradiated region was observed in-situ by EPMA and then ex-situ by a JEM-2000FX TEM operated under 200 kV.

3. Results

3.1 Threshold of electron energy and flux

Fig. 1 shows examples of scanning electron microscopy (SEM) images of the irradiated regions of a pristine a-Ge sample at 1 and 3 keV: the electron flux and energy are (a) $1.4 \times 10^{15}\text{ m}^{-2}\text{ s}^{-1}$ and 1 keV, (b) $2.0 \times 10^{15}\text{ m}^{-2}\text{ s}^{-1}$ and 3 keV, (c) $3.0 \times 10^{15}\text{ m}^{-2}\text{ s}^{-1}$ and 3 keV. The dark square parts correspond to a free-standing film supported by the surrounding Cu grid, shown in bright contrast. Wrinkles often

form in films recovered on the grid after separation from the substrate. The dotted squares in the figures indicate the irradiated area, $8 \times 8 \mu\text{m}^2$. No change in contrast is seen in the SEM image of Fig. 1 (a), indicating that no change in a-Ge due to irradiation occurred. While Fig. 1 (b) is similar to Fig. 1 (a), the contrast in the irradiated region in (b), shown by an arrow, is brighter than the surrounding area. In the irradiated area, coarse crystalline particles of 100-200 nm in diameter appeared as shown in supplemental Fig. 1, but crystallization was limited to the $8 \times 8 \mu\text{m}^2$ irradiated region. In contrast, the SEM image of Fig. 1(c) shows a distinctively circular pattern over a wide range exceeding 100 μm in diameter; this pattern is a typical feature of EC^{15-18,25,26)}, which occurs instantaneously when subjected to stimulation. In summary, EC occurred at a threshold flux for the energy of 2 - 20 keV, while it did not at $1.4 \times 10^{15} \text{ m}^{-2} \text{ s}^{-1}$, 1 keV, which is an upper-limit flux output by the EPMA. Explosive crystallization can be induced at $10^{15} - 10^{16} \text{ m}^{-2} \text{ s}^{-1}$ at 2-20 keV, which is 10^5 order of magnitude lower than that of the 100 keV typically used so far.¹⁴⁾

Figure 2 shows the threshold of electron flux, F_t , inducing EC of pristine films of a-Ge. While the threshold decreases with decreasing electron energy from 20 to 3 keV, it increases from 3 to 2 keV. EC did not occur at an upper limit flux of $1.4 \times 10^{15} \text{ m}^{-2} \text{ s}^{-1}$ at 1 keV, as mentioned above.

The cross section for ionization, Q , for K and L shells can be expressed as the following general form^{27,28)}:

$$Q = C \frac{1}{E_x^2} f(E) \quad (1)$$

where E_x and E are the absorption edge energy and the energy of electron beam, respectively, and C is constant. Q is determined by the function $f(E)$ expressed as

$$f(E) = \frac{E_x}{E} \ln \frac{E}{E_x} \quad (2)$$

Figure 3 (a) shows $f(E)$ as a function of E for $E_K = 11.104$ and $E_L = 1.420$ keV of the absorption edge energies of the K and L shells of Ge, respectively.²⁹⁾ The excitation of the K and L shell is highly efficient at 20 keV and 3 keV, respectively, where $f(E)$ is nearly at its maximum value. In contrast, $f(E)$ for the L shell falls to around 0.25 for $E = 2$ and 10 keV, and therefore the excitation of L shell is less efficient than at 3 keV. Because 1 keV is lower than the threshold energy of $E_L = 1.420$ keV, the electron beam does not induce crystallization at 1 keV.

The value of $f(E)$ at 2 keV is nearly equal to that at 10 keV, but F_t at 2 keV is only one-fourth the value of F_t at 10 keV. Figure 3 (b) shows the fraction of electrons absorbed by the 40 nm thick a-Ge film, which was determined as a ratio of transmission current to the incident current. While the absorption fraction is close to 0.1 over 10 keV, it is about 0.5 at 2 keV, indicating that more electrons interact with Ge atoms in the film at 2 keV than at 10 keV. As a result, F_t at 2 keV is lower than F_t at 10 keV. In conclusion, the threshold of electron flux for inducing EC due to electronic excitation effects can be determined both by cross section for ionization and the absorption of electrons. The former indicates the likelihood of ionization per atom, and the latter indicates the number of atoms in an area subject to electron irradiation.

3.2 Crystallization microstructure

Figure 4 shows a typical example of the microstructure of the explosively crystallized region irradiated at 3 keV. Fig. 3 (a) is a SEM image of an overall crystallized region, and Figs. 4 (a-I) and 4 (a-II) correspond to the magnified TEM views of the central region I and outer periphery region II in Fig. 4 (a), respectively. Crystallization occurred radially at the region I (a-I) and spirally at the region II (a-II). These microstructures are similar to those reported previously.¹⁴⁾ Fig. 4(b) shows the selected-area electron diffraction patterns taken from the regions II. The major patterns were all identified as consistent with those of the diamond cubic structure. But, extra diffraction spots α , located at the

position of {222}, is extraordinary, in that this is in principle forbidden in the diamond cubic structure. The extra diffraction spots are due to the superposition of the patterns and double diffraction through a number of planar defects parallel to (111),^{30,31)} which inevitably form due to the extremely rapid crystal growth.

3.3 Effect of aging on explosive crystallization

Figure 5 compares the SEM images of the pristine samples (a,b) and samples aged for 30 months at room temperature (c,d) irradiated at the threshold flux at 3 and 20 keV. EC occurred both in the pristine sample (a,b) and aged sample (c,d) in a nearly identical region, shown by the dotted circles. This is different from the crystallization behavior of a-Ge with continuous heating,¹³⁾ flash-lamp annealing,¹⁴⁾ and electron irradiation at 100 keV.^{11,12,14)} That is, aged samples crystallize not explosively but ordinarily, forming homogeneously fine nanograins 5-10 nm in diameter.

4 Discussion

We demonstrated in this study that EC occurs in pristine a-Ge films when irradiated by an electron beam of 2 - 20 keV at a threshold of flux in the range of 10^{15} - 10^{16} m⁻² s⁻¹, which is 10⁵ orders of magnitude lower than that at 100 keV. The present results indicate that the breaking and rearrangement of unstable bonds in a-Ge caused by the effects of electron excitation seen with a high level of efficiency at low electron energy. It should also be noted that EC occurred even in the samples aged for a long period of time, 30 months. In no other study on other processes has EC been reported to occur in aged samples.¹¹⁻¹⁴⁾

Figure 6 shows possible pathways of the structural transitions of a-Ge in time and mean-square-displacement coordinates, in which the slope represents the average rate of the displacement of atoms in an area subject to stimulation. At a moderate rate, for example, solid line I, crystallization occurs ordinarily via structural relaxation. We reported that when pristine a-Ge films are pre-annealed at

intermediate temperatures below crystallization temperature for hours¹³⁾ or are pre-irradiated at low flux at 100 keV,¹²⁾ they crystallize ordinarily to homogeneously fine nanograins. In contrast, EC occurs in pristine a-Ge films by high-flux electron irradiation at 100 keV and flash-lamp annealing, but not in aged samples subject to aging at room temperature over six months.¹⁴⁾ These cases correspond to rapid atomic-displacement, as shown by dotted line II; pristine samples go directly to EC without any transition in structure. However, because aged samples have experienced a degree of structural relaxation, EC no longer occurs at slope II. Irradiation by electrons at low energy levels, below 20 keV, investigated in this work, is a much faster process than that at 100 keV, as shown by slope III. Atomic displacement occurs so rapidly that EC occurs in not only pristine samples but also aged samples. A key finding in this investigation is related to the number of atoms in an area subject to electron irradiation; a 2-20 keV electron beam was found to stimulate more atoms than one at 100 keV (as discussed in Sect. 3.1), but the rate of atomic displacement due to irradiation at 100 keV is the same as that at 2-20 keV.

We proposed that MRO clusters introduced in sputter-deposited a-Ge behave as nuclei and that their extremely rapid growth is due to the rapid stimulation of the fluid interface of a liquid-like, high-density amorphous state by either electron irradiation at 100 keV or flash-lamp annealing.¹⁴⁾ The number and size of MRO clusters are certainly reduced due to aging at room temperature over several months,¹¹⁾ but some MRO clusters remain in the films. It should be noted that compressive residual stress between the MRO clusters and matrix would assist the formation of the fluid interface of high-density amorphous state.¹⁴⁾ The residual stress would remain to a certain degree even by aging. It was determined that this mechanism can occur even in aged samples subjected to extremely rapid stimulation in the form of electron irradiation at 2- 20 keV. These results indicate that the structural

features are a primary factor and the strength of stimulation is a secondary one for the explosive crystallization of a-Ge.

The present finding has potential industrial applications. A conventional electron-beam lithography technique, equipped with an electron gun of SEM-level energies, can be used to obtain polycrystalline films of Ge not only on glass substrates but also on polymer substrates. This would provide industry with a process with highly desirable characteristic: it has a low thermal-budget, it is energy saving, and it results in negligible damage to substrates. An extension to this investigation of the microstructure of the EC of substrate-free a-Ge is being prepared: a new study on EC of a-Ge films deposited on various substrates is expected to shed further light on the potential of these techniques.

5. Conclusions

In this investigation, it was demonstrated that irradiating a substrate-free amorphous Ge films with an electron beam with SEM-level energies between 2 and 20 keV induces the explosive crystallization. Electron flux required for this phenomenon were approximately $10^{15} - 10^{16} \text{ m}^{-2} \text{ s}^{-1}$ at 2 - 20 keV, which is 10^5 order of magnitude lower than that at 100 keV. Explosive crystallization occurred in not only pristine films but also stabilized samples subject to aging at room temperature for 30 months. This indicates that the most effective factors in explosive crystallization of a-Ge are that the stimulation is both extremely rapid and highly efficient.

Supplementary Material

See supplementary material for TEM images of the irradiated area of a pristine a-Ge sample at $2.0 \times 10^{15} \text{ m}^{-2} \text{ s}^{-1}$, 3 keV, corresponding to Fig. 1 (b).

Acknowledgement

This work was financially supported by the Murata Science Foundation (No. M20-074). We acknowledge financial support by Japan Society for the Promotion of Science (JSPS) KAKENHI (Grant No. 19H02463).

Availability of data

The data that supports the findings of this study are available within the article.

References

- 1) G. Kissinger and S. Pizzini, *Silicon, Germanium, and Their Alloys* (CRC Press, Boca Raton, 2015).
- 2) K. Usuda, Y. Kamata, Y. Kamimuta, T. Mori, M. Koike, and T. Tezuka, *Appl. Phys. Express* 7, 056501 (2014).
- 3) K. Toko, R. Yoshimine, K. Moto, and T. Suemasu, *Sci. Rep.* 7, 16981 (2016).
- 4) A. Toriumi and T. Nishimura, *Jpn. J. Appl. Phys.* 57, 010101 (2018).
- 5) K. Toko, I. Nakao, T. Sadoh, T. Noguchi, and M. Miyao, *Solid-State Electron.* 53, 1159 (2009).
- 6) S. Kabuyanagi, T. Nishimura, K. Nagashio, and A. Toriumi, *Thin Solid Films* 557, 334 (2014).
- 7) H. Watakabe, T. Sameshima, H. Kanno, and M. Miyao, *Thin Solid Films* 508, 315 (2006).
- 8) W. Yeh, H. Chen, H. Huang, C. Hsiao, and J. Jeng, *Appl. Phys. Lett.* 93, 094103 (2008).
- 9) K. Sakaike, S. Higashi, H. Murakami, and S. Miyazaki, *Thin Solid Films* 516, 3595 (2008).
- 10) N. Matsuo, N. Yoshioka, and A. Heya, *Jpn. J. Appl. Phys.* 56, 085505 (2017).
- 11) M. Okugawa, R. Nakamura, M. Ishimaru, K. Watanabe, H. Yasuda, and H. Numakura, *J. Appl. Phys.* 119, 214309 (2016).
- 12) M. Okugawa, R. Nakamura, M. Ishimaru, H. Yasuda, and H. Numakura, *J. Appl. Phys.*, 120, 134308 (2016).
- 13) M. Okugawa, R. Nakamura, M. Ishimaru, H. Yasuda, and H. Numakura, *AIP Adv.* 6, 125035 (2016).
- 14) M. Okugawa, R. Nakamura, H. Numakura, A. Heya, N. Matsuo, and H. Yasuda, *Jpn. J. Appl. Phys.* 58, 045501 (2019).
- 15) T. Takamori, R. Messier, and R. Roy, *Appl. Phys. Lett.*, 20, 201 (1972).
- 16) L. Nikolova, M. J. Stern, J. M. MacLeod, B. W. Reed, H. Ibrahim, G. H. Campbell, F. Rosei, T. LaGrange, and B. J. Siwick, *J. Appl. Phys.*, 116, 093512 (2014).
- 17) J. R. Parsons and C. W. Hoelke, *Philos. Mag. A* 50, 329 (1985).
- 18) K. Ohdaira and H. Matsumura, *Thin Solid Films* 524, 161 (2012).
- 19) A. Meldrum, L. A. Boatner, and R. C. Ewing, *J. Mater. Res.*, 12, 1816 (1997).
- 20) I. Jenčič, M. W. Bench, I. M. Robertson, and M. A. Kirk, *J. Appl. Phys.* 78, 974 (1995).
- 21) H. Yasuda, *Progress in Advanced Structural and Functional Materials Design*, (Springer, 2013) Chapter 22.
- 22) M. H. Bhat, V. Molinero, E. Soignard, V. C. Solomon, S. Sastry, J. L. Yarger, and C. A. Angell, *Nature* 448, 787 (2007).
- 23) S. Sastry and C. Austen Angell, *Nature Materials* 2, 739 (2003).
- 24) O. I. Barkalov, V. G. Tissen, P. F. McMillan, M. Wilson, A. Sella, and M. V. Nefedova, *Phys. Rev. B* 82, 020507 (2010).
- 25) T. Takamori, R. Messier, and R. Roy, *J. Mater. Sci.*, 8, 1809 (1973).

This is the author's peer reviewed, accepted manuscript. However, the online version of record will be different from this version once it has been copyedited and typeset.
PLEASE CITE THIS ARTICLE AS DOI: 10.1063/1.50052142

- 26) A. Mineo, A. Matsuda, T. Kurosu, and M. Kikuchi, *Solid State Commun.* 13, 329 (1973).
- 27) C. J. Powell, *Rev. Mod. Phys.* 48, 33 (1976).
- 28) T. P. Schreiber and A. M. Wims, *Ultramicroscopy* 6, 323 (1981).
- 29) R. Woldseth, *X-ray energy spectrometry* (Kevex Corporation, Burlingame, 1973).
- 30) C. Cayron, M. Den Hertog, L. Latu-Romain, C. Mouchet, C. Secouard, J.-L. Rouviere, E. Rouviere, and J.-P. Simonato, *J. Appl. Crystallogr.*, 42, 242 (2009).
- 31) M. Okugawa, R. Nakamura, A. Hirata, M. Ishimaru, H. Yasuda, and H. Numakura, *J. Appl. Crystallogr.*, 51, 1467 (2018).

Figure captions

FIG. 1. SEM images of irradiated regions of a pristine a-Ge sample. Electron flux and energy are (a) $1.4 \times 10^{15} \text{ m}^{-2} \text{ s}^{-1}$ and 1 keV (b) $2.0 \times 10^{15} \text{ m}^{-2} \text{ s}^{-1}$ and 3 keV, (c) $3.0 \times 10^{15} \text{ m}^{-2} \text{ s}^{-1}$ and 3 keV. Dotted squares indicate the irradiation area of electron beam, $8 \times 8 \mu\text{m}^2$.

FIG. 2. Threshold of electron flux, F_t , inducing the explosive crystallization of pristine a-Ge.

FIG. 3. (a) $f(E)$ for the K and L shells of germanium according to equation (2) considering the cross section for ionization Q , as expressed in equation (1). (b) Absorption fraction of electrons by a a-Ge films 40 nm in thickness.

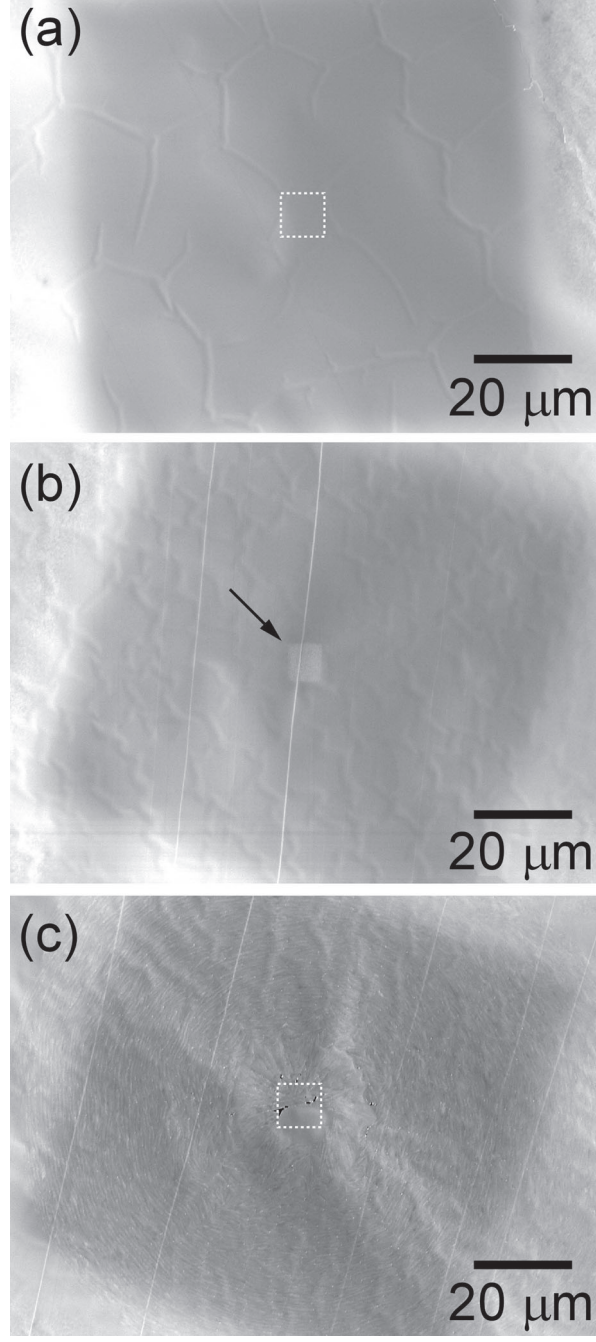
FIG. 4. A typical example of the microstructure of an explosively crystallized region irradiated at 3 keV. (a) SEM image of a completely crystallized region, (a-I), (a-II) TEM images of region I and II in (a), and (b) selected-area electron diffraction patterns corresponding to (a-I) and (a-II).

FIG. 5. SEM images of (a,b) a pristine sample and (c,d) a sample aged for 30 months irradiated by the threshold electron flux at 3 and 20 keV. The dotted circles indicate the boundary of explosive crystallization region as a guide.

FIG. 6. A possible pathway of structural transitions. Mean-square-displacement means average displacement of atoms in an area subject to stimulation.

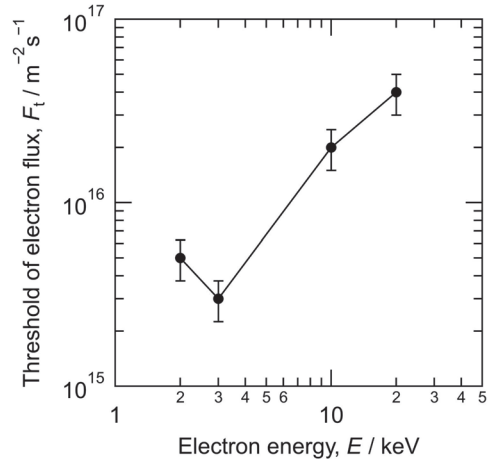
This is the author's peer reviewed, accepted manuscript. However, the online version of record will be different from this version once it has been copyedited and typeset.

PLEASE CITE THIS ARTICLE AS DOI: 10.1063/5.0052142

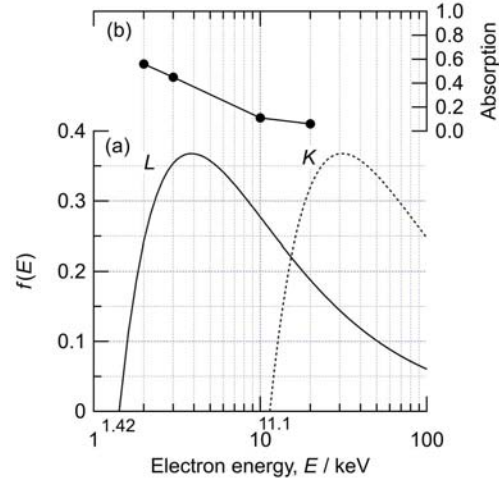


This is the author's peer reviewed, accepted manuscript. However, the online version of record will be different from this version once it has been copyedited and typeset.

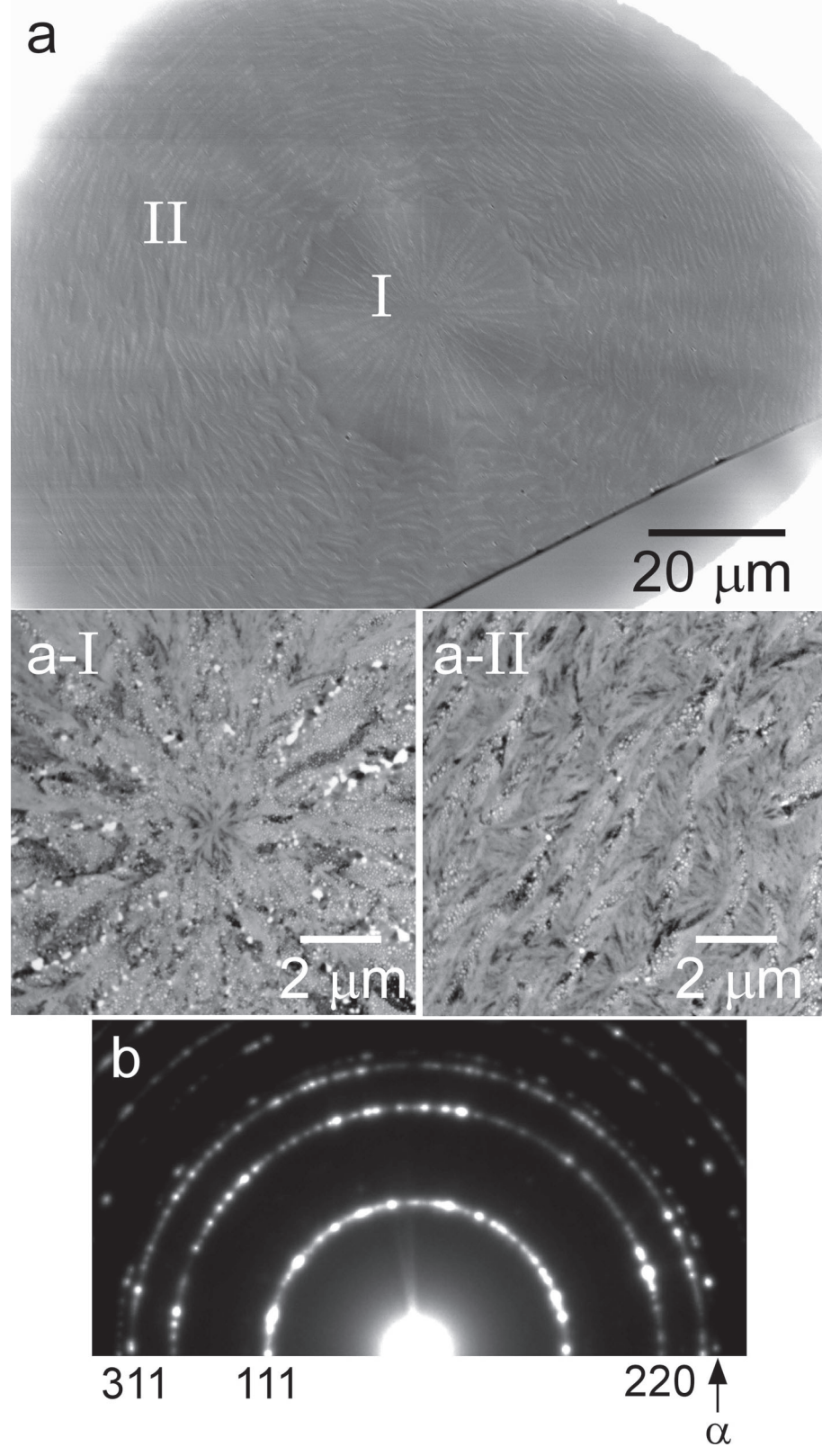
PLEASE CITE THIS ARTICLE AS DOI: 10.1063/5.0052142



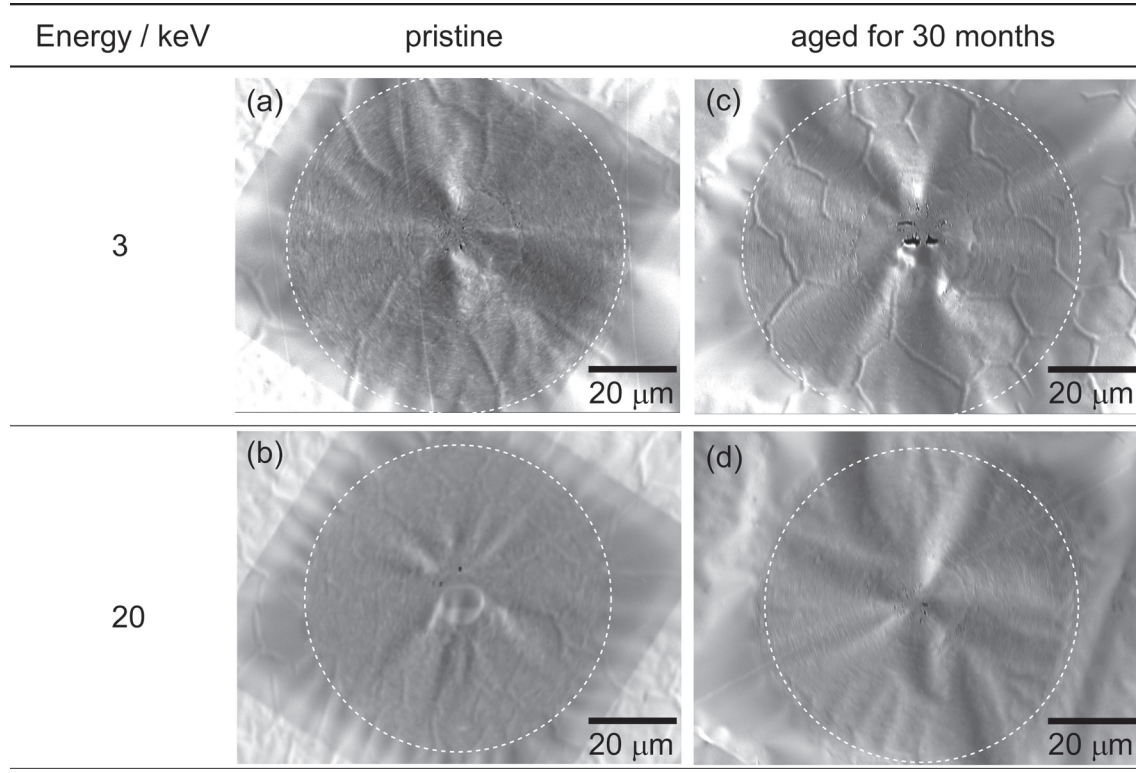
This is the author's peer reviewed, accepted manuscript. However, the online version of record will be different from this version once it has been copyedited and typeset.
PLEASE CITE THIS ARTICLE AS DOI: 10.1063/5.0052142



This is the author's peer reviewed, accepted manuscript. However, the online version of record will be different from this version once it has been copyedited and typeset.
PLEASE CITE THIS ARTICLE AS DOI: 10.1063/5.0052142



This is the author's peer reviewed, accepted manuscript. However, the online version of record will be different from this version once it has been copyedited and typeset.
PLEASE CITE THIS ARTICLE AS DOI: 10.1063/5.0052142



This is the author's peer reviewed, accepted manuscript. However, the online version of record will be different from this version once it has been copyedited and typeset.

PLEASE CITE THIS ARTICLE AS DOI: 10.1063/5.0052142

